Soil Biology and Biochemistry 156 (2021) 108212

Contents lists available at ScienceDirect

Soil Biology and Biochemistry

journal homepage: http://www.elsevier.com/locate/soilbio

Biochar with large specific surface area recruits N_2O-reducing microbes and mitigate N_2O emission

Jiayuan Liao [a,b,1], Ang Hu [a,1], Ziwei Zhao [a], Xiangrong Liu [a], Chu Jiang [d], Zhenhua Zhang [a,c,*]

[a] Southern Regional Collaborative Innovation Center for Grain and Oil Crops in China, College of Resources and Environmental Sciences, Hunan Agricultural University, Changsha, 410128, China
[b] Guangdong Province Key Laboratory for Climate Change and Natural Disaster Studies, School of Atmospheric Sciences, Sun Yat-sen University, Guangzhou, 510275, China
[c] National Engineering Laboratory on Soil and Fertilizer Resources Efficient Utilization, Hunan Provincial Key Laboratory of Farmland Pollution Control and Agricultural Resources Use, Hunan Provincial Key Laboratory of Nutrition in Common University, Changsha, 410128, China
[d] CAS Key Laboratory of Tropical Forest Ecology, Xishuangbanna Tropical Botanical Garden, Chinese Academy of Sciences, Mengla, Yunnan, China

ARTICLE INFO

Keywords:
Biochar
Specific surface area
Nitrogen
N_2O-related functional genes
nosZ
N_2O emission

ABSTRACT

Bacteria and archaea colonizing on biochar have been reported to possess nitrogen-metabolizing abilities. A larger specific surface area of biochar may enhance the activities of nitrous oxide (N_2O)-reducing microbes, thereby mitigating N_2O emission; however, the underlying mechanisms remain unclear. A 56-day incubation assay was performed with five treatments: no addition, urea only, and addition of three types of biochars (with different specific surface areas: 1193, 2023, and 2773 $m^2\ g^{-1}$) combined with urea. N_2O emission increased with the specific surface area of biochar up to 2023 $m^2\ g^{-1}$ and decreased thereafter by 37% as compared with the urea only addition. By increasing soil pH, C/N ratio, nitrogen availability, and cation exchange capacity, the biochar with the largest specific surface area decreased soil N_2O emission by affecting the diversity, abundance, and composition of total bacteria and N_2O-producing microbial communities. A larger specific surface area of biochar correlated with a higher abundance of nitrogen-fixing (*nifH*), -nitrifying (*amoA*), and -denitrifying (*nirK*, *nirS*, and *nosZ*) genes. An increased abundance of ammonia-oxidizing bacteria and archaea, in the biochar with a smaller specific surface area, resulted in higher N_2O emission. As the abundance of *nosZ* increased, the addition of the biochar with the largest specific surface area resulted in a higher ratio of *nosZ*/(*amoA* + *nirS* + *nirK*), leading to decreased N_2O emission. Furthermore, the abundance of *nifH*, *amoA*, *nirK*, and *nosZ* on biochar (extraction from soil after 56-day incubation) was positively correlated with that in soil. Thus, the relative specific surface area of biochar should be taken into consideration when using it in agriculture, as our results show that biochars with larger specific surface areas decrease N_2O emission by recruiting N_2O-reducing microbes and upregulating the abundance of nitrogen-fixing, -nitrifying, and -denitrifying genes.

1. Introduction

Nitrous oxide (N_2O) is one of the most prominent greenhouse gases that leads to global warming and ozone layer depletion in the stratosphere (Ravishankara et al., 2009). Croplands are the main anthropogenic source of atmospheric N_2O worldwide (Shcherbak et al., 2014; Zhu et al., 2015; Wang et al., 2020). Increased use of nitrogenous fertilizers in croplands accounts for 80% of the global increase in terrestrial N_2O emission and resulted in accelerated global warming over the last century (Galloway et al., 2008; Tian et al., 2019).

Biochar is a carbon-rich material produced by the pyrolyzation of biomass under high temperature, with limited oxygen (O_2) supply (Atkinson et al., 2010). Biochar has been suggested for use as a cost-effective agricultural management practice to decrease N_2O emission from croplands (Van et al., 2010; Case et al., 2012; Huang et al., 2013; Cayuela et al., 2014). In soil, N_2O is generated *via* microbial nitrification and denitrification (Liu et al., 2016). While the ammonia monooxygenase encoding gene *amoA* is the pivotal functional gene for

* Corresponding author. Southern Regional Collaborative Innovation Center for Grain and Oil Crops in China, College of Resources and Environmental Sciences, Hunan Agricultural University, Changsha, 410128, China.
E-mail address: zhzh1468@163.com (Z. Zhang).
[1] These authors contributed equally to this work.

https://doi.org/10.1016/j.soilbio.2021.108212
Received 9 May 2020; Received in revised form 27 January 2021; Accepted 6 March 2021
Available online 13 March 2021

nitrification, the nitrite reductase encoding genes *nirK* and *nirS* and the nitrous oxide reductase encoding gene *nosZ* are involved in denitrification (Xu et al., 2018). Biochar affects microbial nitrification and denitrification by changing the physical and chemical properties of soil, eventually inhibiting N_2O emission (Spokas et al., 2010; Zhang et al., 2010; Lin et al., 2017). Biochar application decreases N_2O emission through several mechanisms: (i) inhibiting nitrification and, thus, the formation of N_2O *via* ethylene (Spokas et al., 2010); (ii) improving soil aeration to decrease the rate of denitrification (Yanai et al., 2007); (iii) reducing substrate availability for denitrification by adsorbing NO_3^- (Van et al., 2010); (iv) adsorbing N_2O (Cornelissen et al., 2013); and (v) increasing the activities of N_2O-reducing microbes by elevating soil pH (Van et al., 2010). For instance, biochar addition decreases N_2O emission by increasing *nosZ* gene abundance owing to increase in the pH of acidic upland soil (Xu et al., 2014). Previous studies have mainly focused on N_2O-reducing microbial processes in soils to explain the mechanisms underlying the beneficial effects of biochar, whereas very few studies have examined the specific interactions between biochar surface and these microbes. Therefore, a better understanding of the mechanisms of action of N_2O-reducing microbes on biochar surfaces is of great importance for addressing N_2O emission.

Different functional groups, such as carboxyl and hydroxyl groups, lactones, chromenes, and ketones, in porous biochar can substantially adsorb ammonium and nitrate (Schmidt et al., 2015; Kammann et al., 2015). These substrates support the recruitment of diverse microbial communities, and the biochar itself serves as an optimal shuttle for microbial electron transfer and redox reactions (Kappler et al., 2014; Saquing et al., 2016; Yuan et al., 2019). The porous structure of biochar facilitates microbial colonization, which drives a series of biological processes in the nitrogen cycle, generating N_2O (Yu et al., 2015; Zhou et al., 2016; Dai et al., 2017; Ye et al., 2017). We hypothesized that N_2O-reducing microbes colonizing biochar surfaces contribute to reducing N_2O emission. High-throughput sequencing, quantitative PCR (qPCR), and fluorescence *in situ* hybridization (FISH) analyses of nitrification (ammonia oxidizing bacteria (AOB) and ammonia oxidizing archaea (AOA) *amoA*) and denitrification (*nirK*, *nirS*, and *nosZ*) functional genes involved in N_2O emission were performed using biochar with different specific surface areas (SSAs). The objectives of this study were as follows: (i) to evaluate the effects of adding biochar with different SSAs on N_2O emission; (ii) to identify the N_2O-reducing bacteria (*nosZ*) and determine the composition of the microbial community in the presence of biochar; (iii) to determine whether *amoA*, *nirS*, *nirK*, *nosZ*, and *nifH* were detected on biochar; and (iv) to study whether the abundance of these genes found on biochar is related to N_2O reduction.

2. Materials and methods

2.1. Soil sampling

Topsoil samples (0–20 cm) were taken from a paddy field in Anren County, Hunan Province in southern China (26°17′N–26°50′N, 113°05′E–113°36′E). The sampling field had been managed *via* long-term crop rotation (rice–rice–oilseed rape rotation) for the last 30 years (Lu et al., 2018). Table S1 shows the chemical properties of the topsoil before the experiment. Soil samples were collected after surface organic residues were removed, and the samples were then air-dried, ground to pass through a 2-mm sieve, and thoroughly homogenized.

2.2. Biochar preparation

To attract more microbes to the biochar surface, we used potassium hydroxide (KOH) to increase the surface area of biochar (Liang et al., 2008; Dai et al., 2017). Three types of biochar with different SSAs were derived from oilseed rape straws collected from the field station at Hunan Agricultural University. The oilseed rape straws were air-dried and ground into particles with size <0.3 mm. Under a 3 L min^{-1} N_2 flow, straws were pyrolyzed at 400 °C for 3 h (as precursors for the biochars with different SSAs) in a laboratory-scale pyrolysis unit comprising a tube reactor equipped with a programmable temperature controller (Liu et al., 2019). After the reactor was cooled to room temperature (25 °C), KOH was mixed with the precursor in three proportions (precursor: KOH = 1:1, 1:2, and 1:3), and then activated for 3 h in the reactor at 700 °C, cooled down, washed with sterile water to a pH = 7, and naturally air-dried on an airflow pressure aseptic operating table (Liang et al., 2008). These three products were referred to as biochar1 (B1), biochar2 (B2), and biochar3 (B3) [rank of SSA: B3(2773 m^2 g^{-1}) > B2(2023 m^2 g^{-1}) > B1(1193 m^2 g^{-1})]. The physicochemical and morphological characteristics of these biochar types are summarized in Table S2 and Fig. 1.

2.3. Incubation setup

The incubation assay was performed as described by Lin et al. (2017), with some modifications. Briefly, 20 g air-dried soil samples were added into each of a series of 100-mL Erlenmeyer flasks and maintained at approximately 50% maximum water holding capacity, using distilled water, according to the method of Laird et al. (2010). All flasks were covered with aluminum foil having needle-punched holes to maintain aerobic conditions and incubated at 25 °C in the dark for three days to activate the microorganisms. Five experimental groups with a randomized complete block design were set up: no addition (Control), urea only (+N), and three kinds of SSA biochar combined with urea (NB1, NB2 and NB3). Urea was applied at a rate of 200 mg N kg^{-1} (total of 150 flasks), while the biochar addition rate was 4% of the oven-dried soil mass, which was equivalent to a field application rate of 80 t ha^{-1} in a 0–20 cm plowed layer. The added biochar was thoroughly mixed with the soil using a glass rod. All flasks were covered with perforated aluminum foil and incubated at 25 °C in the dark for 56 days. To maintain the soil water content, deionized water was added with a mini pipette every other day throughout the incubation period.

N_2O flux was measured according to the methods of Harter et al. (2014) and Lin et al. (2017). Three replicate flasks of each experimental group were used to measure N_2O fluxes after 1, 3, 5, 7, 10, 14, 21, 35, and 56 days of incubation. Before gas sampling, the headspace air in the flasks was flushed with fresh air. The flasks were capped immediately with silicone rubber stoppers. An additional 20 mL of fresh air was injected into the flasks using a syringe and thoroughly mixed with the headspace gas. The same volume of gas was sampled and injected into pre-evacuated vials, which served as the time-zero sample for the analysis. The flasks were then incubated for 2 h and 20 mL of headspace gas was sampled from these flasks. After gas sampling, the stoppers were removed and aluminum foil was used to cover the flasks again. N_2O concentration was measured using a gas chromatograph (GC; Agilent 7890, Agilent Technologies, Santa Clara, CA, USA) equipped with an electron capture detector. The GC setup and configuration have been described in detail previously (Loftfield et al., 1997). Gas fluxes were calculated using the slope of the temporal change in concentration in the closed bottle according to the equations published by Ruser et al. (1998).

For soil sampling, three replicates of each experimental group (a total of 15 bottles) were sampled destructively every time. Samples (20 g) from each bottle were poured into individual sterile Petri dishes and thoroughly homogenized after microcosm setup. After 1, 3, 7, 14, 21, 35, and 56 days of incubation, 5 g of the samples was stored at −80 °C for DNA extraction, qPCR, or high-throughput sequencing, whereas the remaining 15 g was used for analyses of soil chemical properties.

For biochar particle sampling, three replicates of each experimental group (a total of 15 bottles) were sampled after 56 days of incubation (hereafter called post-B1, post-B2, and post-B3) according to the modified protocol of Lin et al. (2012). First, 20 g of soil-biochar mixtures of the experimental groups were poured into individual sterile beakers, and then 100 mL sterile water was added to each beaker, followed by

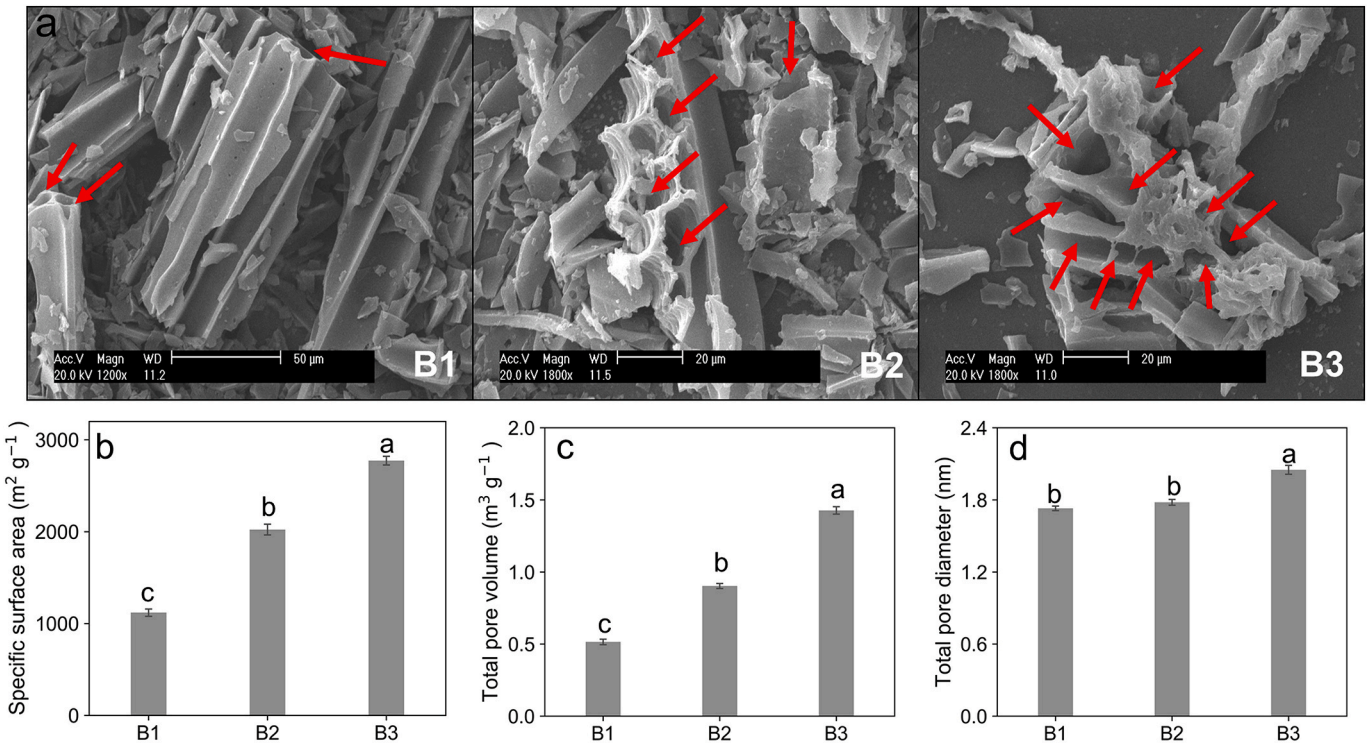

Fig. 1. Scanning electron micrograph (SEM) (a), specific surface area (b), total pore volume (c) and total pore diameter (d) of different biochars (biochar1: B1, biochar2: B2, and biochar3: B3). Red arrows in panel (a) show the porous structure of biochar that serves as a potential habitat for microorganisms. (For interpretation of the references to color in this figure legend, the reader is referred to the Web version of this article.)

gentle stirring for 2 min, and finally, the isolated biochar in the suspension was collected on a sieve during agitation; thus, the biochar particles remained on the sieve surface, while the soil particles passed through it. Finally, biochar particles were collected manually, then gently rinsed with sterile water to remove residual soil particles (soil particles that could not be removed were considered as the biochar-sphere) (Dai et al., 2017), and stored at −80 °C for DNA extraction for qPCR and high-throughput sequencing.

2.4. Soil chemical properties

Soil pH was determined in a 1:5 (w:v) soil-to-water slurry using a pH-meter (AB150, Fisher Scientific, USA). The organic matter content of the soil was determined using an oxidation method with potassium dichromate. The total nitrogen content of soil samples was determined using an automatic azotometer (KDN-102F, Qianjian Ltd., Shanghai, China). Soil NH_4^+−N and NO_3^-N were extracted using 2 M KCl solution at a soil/water ratio of 1:5 at 25 °C and measured on a Smart Continuous-Flow Analyzer (SmartChem200, Shenzhen, China). Total phosphorus was measured using sodium hydroxide fusion, followed by colorimetric analysis. Olsen phosphorus was extracted using 0.5 M $NaHCO_3$ and quantified colorimetrically (Lu et al., 2018). Total potassium was measured using flame photometry after sodium hydroxide fusion, and the available potassium was extracted with NH_4OAc and quantified using flame photometry. Cation exchange capacity was measured with strontium chloride ($SrCl_2$), as described by Calvelo et al. (2015).

2.5. DNA extraction, PCR amplification, and high-throughput sequencing

DNA extractions were carried out in triplicate for each sample (a total of 15 samples) at different time points (after 1, 3, 7, 14, 21, 35, and 56 days of incubation). Of note, DNA extracted on day 56 was used for high-throughput sequencing, while qPCR was performed to determine the functional marker genes at all time points. Total DNA was extracted from biochar particles and soils, using the PowerSoil DNA isolation kit (MO BIO Laboratories, Carlsbad, CA, USA), according to the manufacturer's instructions. Although the kit has a loading capacity of 0.5 g soil, an equivalent weight of biochar particles could not fit the test tube due to their low specific weight. Therefore, 0.1 g biochar particles was used, which led to sufficient DNA yield for subsequent analysis (Ye et al., 2017). DNA concentration was determined by spectrophotometry (NanoDrop One, Thermo Scientific, Waltham, MA, USA), and the quality was assessed using 1.0% (w/v) agarose gel electrophoresis. Finally, 1 mL DNA extracts of each sample were stored at −80 °C for future use.

The V3/V4 regions of the 16S ribosomal RNA (16S rRNA) gene were amplified using PCR (initial denaturation at 98 °C for 2 min, followed by 30 cycles at 98 °C for 30 s, 50 °C for 30 s, and 1 min at 72 °C, with a final extension at 72 °C for 5 min) using the primers 338F (5′-ACTCCTACGGGAGGCAGCA-3′) and 806R (5′-GGACTACHVGGGTWTCTAAT-3′), which target conserved sequences in the bacterial genome. PCR amplification was performed in a 50-μL reaction mixture containing 10 μL 5 × FastPfu Buffer, 2 μL 2.5 mM dNTPs, 1.5 μL of each primer (10 μmol), 0.2 μL Q5 High-Fidelity DNA Polymerase (Sangon Biotech, China), and 40 ng template DNA. The PCR products were extracted from the agarose gel following electrophoresis (1.8% (w/v) agarose) and purified using a MinElute® PCR Purification Kit (Sangon Biotech, China). Finally, all PCR products were quantified by Quant-iT™ dsDNA High-Sensitivity Reagent (Thermo Fisher, Waltham, Massachusetts, USA) and pooled. High-throughput sequencing of the V3/V4 region of bacterial 16S rRNA genes was performed on the purified pooled sample, using the Illumina HiSeq 2500 platform (2 × 250 paired ends), at Biomarker Technologies Corporation, Beijing, China.

Raw FASTQ files were demultiplexed and quality-filtered using QIIME (version 1.17). Operational taxonomic units (OTUs) were clustered with 97% similarity cutoff using UPARSE (Edgar, 2013), and chimeric sequences were identified and removed using UCHIME (Edgar et al., 2011). The taxonomy of each 16S rRNA gene sequence was assigned using an RDP classifier against the SILVA 16S rRNA database

(version 138.1) with a confidence threshold of 70% (Vestergaard et al., 2017; Schöler et al., 2017). Principal component analysis (PCA) was used to visualize the Bray-Curtis dissimilarity matrices based on the OTU data. Heatmaps were used to display the abundance of species in the different samples using the "vegan" package in R (version 4.0.3, http://www.r-project.org/) (Oksanen et al., 2016).

2.6. qPCR

qPCR was performed to determine the functional marker genes (*amoA*, *nifH*, *nirK*, *nirS*, and *nosZ*) using SsoAdvanced™ SYBR® Green Supermix (Bio-Rad Laboratories, Hercules, CA, USA). Each sample was quantified in triplicate using a CFXCONNECT Real-Time PCR Detection System (Bio-Rad Laboratories, Hercules, CA, USA) and gene-specific primers adapted from those used in previous studies. Details of the gene-specific qPCR primers of AOA *amoA* (Francis et al., 2005), AOB *amoA* (Rotthauwe et al., 1997), *nirK* (Henry et al., 2005), *nirS* (Throback et al., 2004), *nosZ* (Kloos et al., 2001), and *nifH* (Marusina et al., 2001; Gaby and Buckley, 2012) are summarized in Table S3.

The functional marker gene amplicons from soil-derived DNA were gel-purified using an OMEGA quick PCR (Sangon Biotech, China) purification kit and ligated into the pMD™19 T-vector (Takara), then further transformed into *Escherichia coli* competent DH5α cells (Takara). The positive white clones were selected for plasmid DNA extraction using an OMEGA Plasmid Extraction Kit and used as functional gene standards. Standard curves were constructed with plasmids containing cloned gene fragments. Results with correlation coefficients and amplification efficiencies, which are summarized in Table S4, were used for downstream analyses (Keshri et al., 2015). All amplified samples were examined on an agarose gel after PCR to confirm successful amplification, and the specificity of the amplification products was confirmed by melting curve analysis.

2.7. FISH

The detected OTUs (for the *nosZ*) in biochar were assayed for the presence of bacterial cells using FISH, as detailed by Amann (1995), adopting fluorescently labeled oligonucleotide probes and relevant oligonucleotide competitors (Epsilon Biological Technology, Beijing, China). A general probe (EUBmix, a combination of EUB338, 338I, and 338II) was selected to target all bacteria, while the specific probe HGC69a was used to detect Actinobacteria (Wendeberg, 2010). Hybridization was conducted for 1.2 h on the slides after dehydration in an ethanol gradient (50, 80, and 98%). DakoR Pen (Glostrup, Denmark) was used to create a hydrophobic barrier when performing FISH on the Superfrost slides. The probes were washed, as detailed by Amann (1995). The samples were rinsed with a pre-warmed washing buffer at 48 °C, and the slides were immersed in this washing solution for 10 min. The slides were airflow dried, mounted using the anti-fading medium Vectashield® (Vector Laboratories Inc., Burlingame, CA, USA), covered with 5 × 2.4 cm coverslips (0.1 mm thickness), and sealed with nail polish. After hybridization, the samples were airflow dried and mounted according to Pernthaler and Pernthaler (2007). Hybridized samples were observed with an epifluorescence microscope (Nikon Corporation, Tokyo, Japan) equipped with a UV lamp (filter sets: DAPI, EX340-380; 118 TRITC, EX540/25). The software NIS-Elements BR 4.30 was used for image processing.

2.8. Statistical analysis

We determined the statistical significance of changes in soil properties and N_2O emissions caused by each treatment. Significant changes in the functional gene copy numbers measured by qPCR under different treatments were compared by ANOVA, using a GLIMMIX model, to determine the differences in the effects of the treatments over time through repeated measurements; $p < 0.05$ was generally considered to indicate statistically significant differences unless otherwise stated. Additionally, the changes in α-diversity (including the Chao1 estimator and Shannon diversity) of the bacterial community due to different treatments were also determined. Regression analyses were used to test the significance of statistical associations between N_2O flux and functional gene abundance in soil and biochar. The significance of the regression coefficients was calculated by Student's *t*-test. Relationships between gene abundance or N_2O emission and soil chemical properties were assessed by correlation analysis (Spearman's rank correlation test). All analyses were performed using the SPSS Statistics version 20.0 software (Armonk, NY, USA). The figures were created using Origin 9.0 (Origin Lab) and Python 3.0 software.

3. Results

3.1. Physicochemical and morphological characteristics of biochar

The main physicochemical properties of the biochar used in the present study are listed in Table S2. The ash, elemental (C, H, and O), and nutrient (N, P, and K) contents were similar among B1, B2, and B3. Scanning electron micrograph showed that B3 had a more porous structure than B2 and B1 (red arrow, Fig. 1a). The SSA, total pore volume (V_T), and total pore diameter (D_p) were in the following order: B3 > B2 > B1(Fig. 1b-c).

3.2. Nitrous oxide emissions

Nitrous oxide emission appeared most rapidly from soil treated with the smallest SSA biochar, preceding the N_2O emissions from urea only and mid-range SSA biochar-treated soils by two and four days, respectively, followed by soil treated with the largest SSA biochar. The quantity of N_2O emission was inversely related to biochar SSA, i.e. biochar with the smallest SSA (3055 μg N $m^{-2}{\cdot}h^{-1}$) > biochar with mid-range SSA (2272 μg N $m^{-2}{\cdot}h^{-1}$) > urea only (1788 μg N $m^{-2}{\cdot}h^{-1}$) > biochar with the largest SSA (1068 μg N $m^{-2}{\cdot}h^{-1}$).

After 56 days of incubation, the cumulative N_2O emission (Fig. 2b) from urea and biochar-treated soils was greater than that in the no addition group, and the highest N_2O emission (578.7 mg m^{-2}) was observed in the smallest SSA biochar-treated soil, which was up to 1.6-times the amount in the urea only treated soil. Biochar with mid-range SSA addition also increased N_2O emissions by 45% relative to the urea only addition, while biochar with the largest SSA decreased N_2O emission by 37% compared with the urea only addition.

3.3. Soil pH and inorganic N

Soil pH was significantly affected by the urea and biochar treatments (Fig. S1). The urea only treatment decreased soil pH on all incubation days, except on day 3. The soil pH slowly decreased after biochar treatment but was higher than the values observed in the urea only and no addition treatment groups during the entire incubation period.

Soil NH_4^+-N content increased with the addition of nitrogenous fertilizer, but decreased more quickly during the first 14 days, reaching a constant level after day 14, as compared to that in the no addition group (Fig. 2c). On the contrary, soil NO_3^--N content increased rapidly until day 14 of incubation and remained constant throughout the incubation period in urea only and biochar treated soils, with the levels being higher than that in the no addition group (Fig. 2d). The NO_3^--N content in the soil treated with biochar having SSA >2023 $m^2\ g^{-1}$ was lower than those in the soils treated with biochars having SSAs ≤2023 $m^2\ g^{-1}$ and the urea only-treated soils after day 7. In nitrogenous fertilizer treated soils, there was an accelerated decrease in NH_4^+-N content coupled with an increase in NO_3^--N content during the first 14 days.

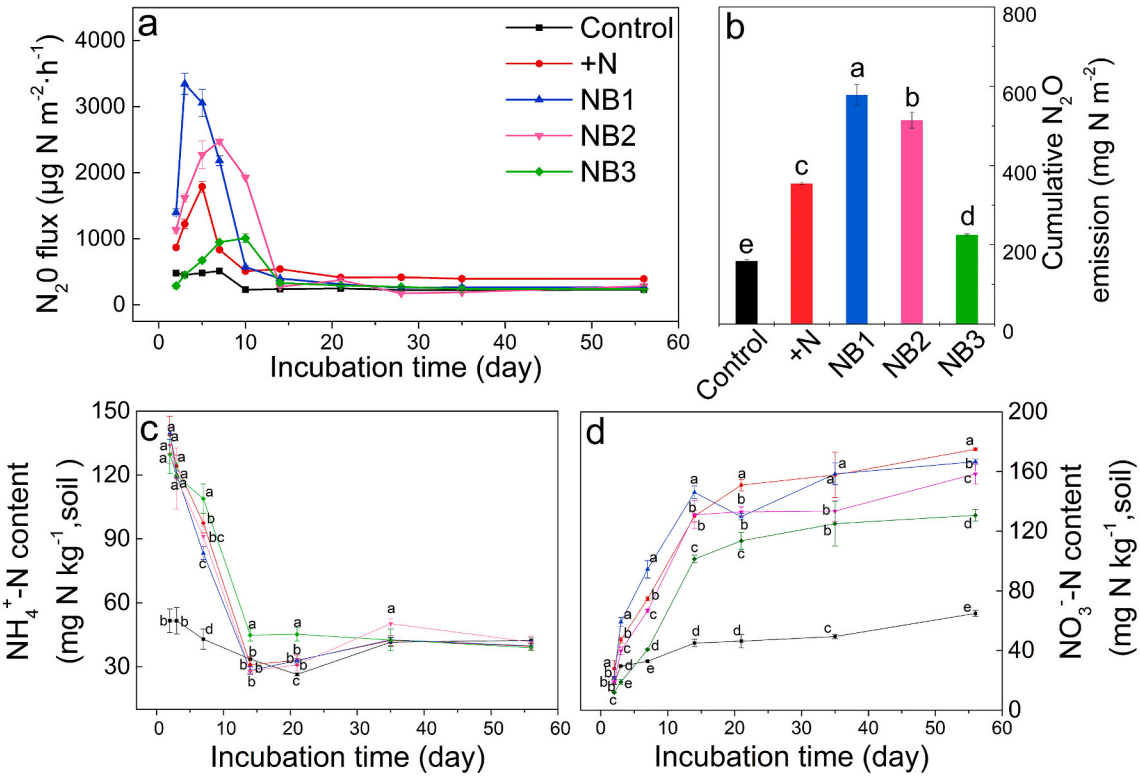

Fig. 2. Temporal (a), cumulative (b) N_2O emissions, dynamic variation of NH_4^+ (c) and NO_3^- (d) contents in five experimental groups during 56 days of incubation. Statistically significant differences among treatments are represented by different lowercase letters ($p < 0.05$). No addition (Control), urea only (+N), and three kinds of SSA combined with urea (NB1, NB2 and NB3).

3.4. Effects of nitrogen and biochar addition on bacterial community composition in soil

PCA analysis of OTUs revealed significant variations in the bacterial community compositions among the different soil samples (Fig. 3a). The first axis, PCA1, explained 62.5% of the variation in the OTU data, PCA2 explained 22.6% of the variation, and the cumulative contribution rate was 85.1%. The bacterial community in the no addition and urea only treated group was separated from those in the biochar treated groups by PCA1. The bacterial α-diversity (Shannon index) for urea only and biochar-treated soils were found to be lower than that for soil with no addition (Fig. 3b). However, the Chao 1 index for biochar with the largest SSA treated soil was higher than those for urea only treated and no addition soils (Fig. 3b).

The most abundant phyla were Proteobacteria, Gemmatimonadetes, Actinobacteria, Acidobacteria, Bacteroidetes, Chloroflexi, Firmicutes, Verrucomicrobia, Planctomycetes, and WPS-2; these taxa accounted for more than 91% of the bacterial sequences in all soils (Fig. 3c). At the phylum level, biochar application increased the relative abundances of Fibrobacteres, Gemmatimonadetes, Rokubacteria, Nitrospirae, Bacteroidetes, and Proteobacteria (Fig. S2). At the OTU level, the abundances of more than half of these taxa were increased by biochar, while the abundances of more than half were lower than those in the urea only treated and no addition soils, although no significant variation between no addition and urea only treated soils was observed (Fig. 3d). Using CCA analysis, we found that biochar addition changed the bacterial community composition by affecting the soil chemical properties, including soil pH, NH_4^+ and NO_3^- content, C/N ratio, and cation exchange capacity (Fig. S3a). Similarly, N_2O flux showed a significant correlation with soil pH, NH_4^+, NO_3^-, C/N ratio, and cation exchange capacity (Fig. S3b).

3.5. Effects of nitrogen and biochar addition on nitrifier community composition in soil

Biochar with different SSAs affected the community composition of archaea harboring *amoA* in the soil, whereas there was no significant change in the community composition of bacteria harboring *amoA* (Fig. S4). The community of archaea harboring *amoA* in urea only treated soil was different from those in the biochar treated soils, and soil treated with biochar having SSA >2023 m^2 g^{-1} was distinguished from those treated with SSA <2023 m^2 g^{-1} by PCA1. PCA1 and PCA2 did not distinguish the communities when the SSA of biochar was <2023 m^2 g^{-1}.

3.6. Dominant OTU of nosZ in soil and localization on the biochar

The community composition of microbes harboring *nosZ* showed a significant difference between urea only and biochar treated soils (Fig. 4a). The relative abundances of the dominant OTUs of *nosZ* were affected by the addition of biochar with different SSA (Fig. 4b). The relative abundance of OTU5 was the highest in the largest SSA biochar-treated soil (Fig. 4b). We investigated the physical localization of OTU5 using FISH and found that it increased with biochar SSA and was particularly visible in the biochar with the largest SSA (red region in Fig. 4c).

3.7. Bacterial community composition in biochar

Biochar particles were extracted from soil after 56 days of incubation. 16S-rRNA high-throughput sequencing revealed the bacterial community in biochar (Fig. S5). PCA of the OTUs showed that the bacterial community composition in biochar varied significantly among biochars with different SSAs (Fig. S5a). The most abundant phyla were Proteobacteria, Gemmatimonadetes, Actinobacteria, Acidobacteria,

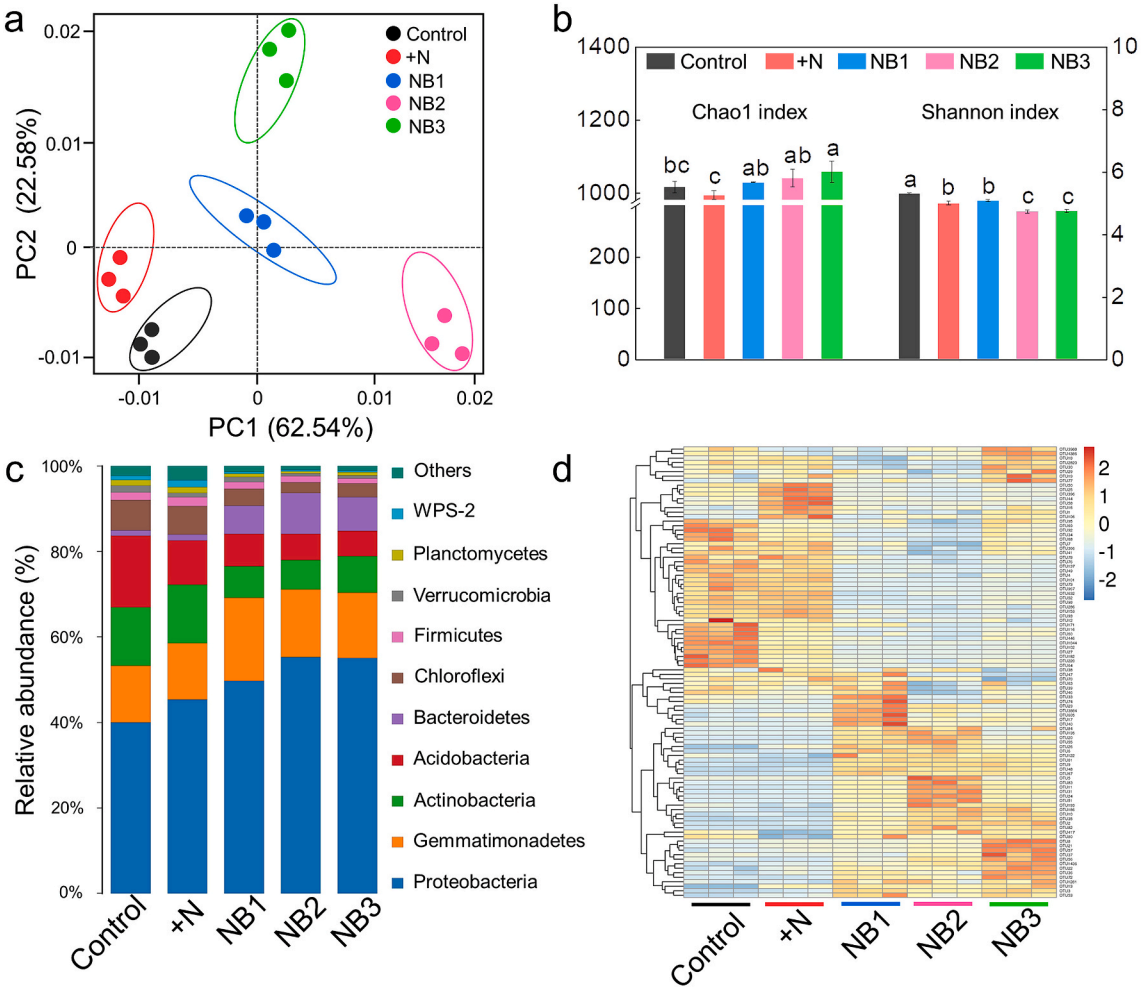

Fig. 3. Bacterial community compositions among different experimental groups. Principal component analysis (PCA) of bacterial community based on 16S-rRNA gene (a). Alpha diversity indices (i.e., Chao1 and shannon) of bacterial community (b). Relative abundances of bacterial phyla. "Other" refers all other taxa with abundances lower than 0.9% (c). The relative abundance of OTUs and their cluster analysis in different treatments as visualised by heatmaps (d). The color intensity of the scale indicated the relative abundance of each OTU. Relative abundance was defined as the number of sequences affiliated with that taxon divided by the total number of sequences per sample (%). No addition (Control), urea only (+N), and three kinds of SSA combined with urea (NB1, NB2 and NB3). (For interpretation of the references to color in this figure legend, the reader is referred to the Web version of this article.)

Bacteroidetes, Chloroflexi, Firmicutes, Verrucomicrobia, Planctomycetes, and WPS-2, similar to those in soil (Fig. S5b).

3.8. Nitrogen-cycling functional gene abundance in soil and biochar

The abundance of N_2O-reducing bacteria was measured by determining the copy numbers of *nosZ* (Fig. 5a). The abundance of *nosZ* in soil increased with an increase in the SSA of biochar during the first 14 days and was the highest in the largest SSA biochar-treated soil. The ratio of the functional genes was investigated to determine the dominant functional genes for nitrification and denitrification. The ratios of *nosZ*/(AOA *amoA* + AOB *amoA*), *nosZ*/(*nirS* + *nirK*), and *nosZ*/(AOA *amoA* + AOB *amoA* + *nirS* + *nirK*) in the largest SSA biochar-treated soil were higher than those in all other soils on day 5 (Fig. 5).

The abundances of AOA *amoA* and AOB *amoA* in the largest SSA biochar-treated soil were higher than those in the other soils on days 14 and 56 (Fig. S6). The abundances of *nirK* and *nirS* were increased upon biochar addition after 7 days of incubation, except *nirS* on day 35 and day 56 (Fig. S6). Over the whole incubation period, *nifH* copy numbers were higher in the largest SSA biochar-treated soil than in other soils except on day 14 (Fig. S6).

Biochar particles were extracted from the soil after 56 days of incubation. qPCR results indicated that nitrogen-cycling functional gene presence varied between different biochars (Fig. 6). The number of nitrogen-cycling functional genes (except the abundance of AOB *amoA*) increased with the SSA of biochar up to 2773 $m^2\ g^{-1}$.

3.9. Relationship between N_2O emission and functional marker gene abundance in soil and biochar

The abundance of nitrogen-cycling functional genes in biochar had positive relationships with the SSA, pore volume, and pore diameter of biochar (Fig. 7a–c). Except for the *nirS*, the abundance of AOA *amoA*, AOB *amoA*, *nirK*, *nosZ*, and *nifH* in microbes found on the biochar showed a positive correlation with that of genes in soil (Fig. 7d).

Regression analysis revealed that N_2O flux positively correlated with AOA *amoA* and AOB *amoA* abundance ($R^2 = 0.24$, $p < 0.05$; $R^2 = 0.32$, $p < 0.05$) (Fig. 8 a-b). However, N_2O flux decreased with an increase in the ratios of *nosZ*/(AOA *amoA* + AOB *amoA*), *nosZ*/(*nirS* + *nirK*), and *nosZ*/(AOA *amoA* + AOB *amoA* + *nirS* + *nirK*) (Fig. 8 c-e). The total N_2O emission decreased with increased *nosZ* abundance in biochar ($R^2 = 0.50$, $p < 0.05$) (Fig. 8 f).

4. Discussion

Biochar enhanced nitrification, and the biochar with the largest SSA

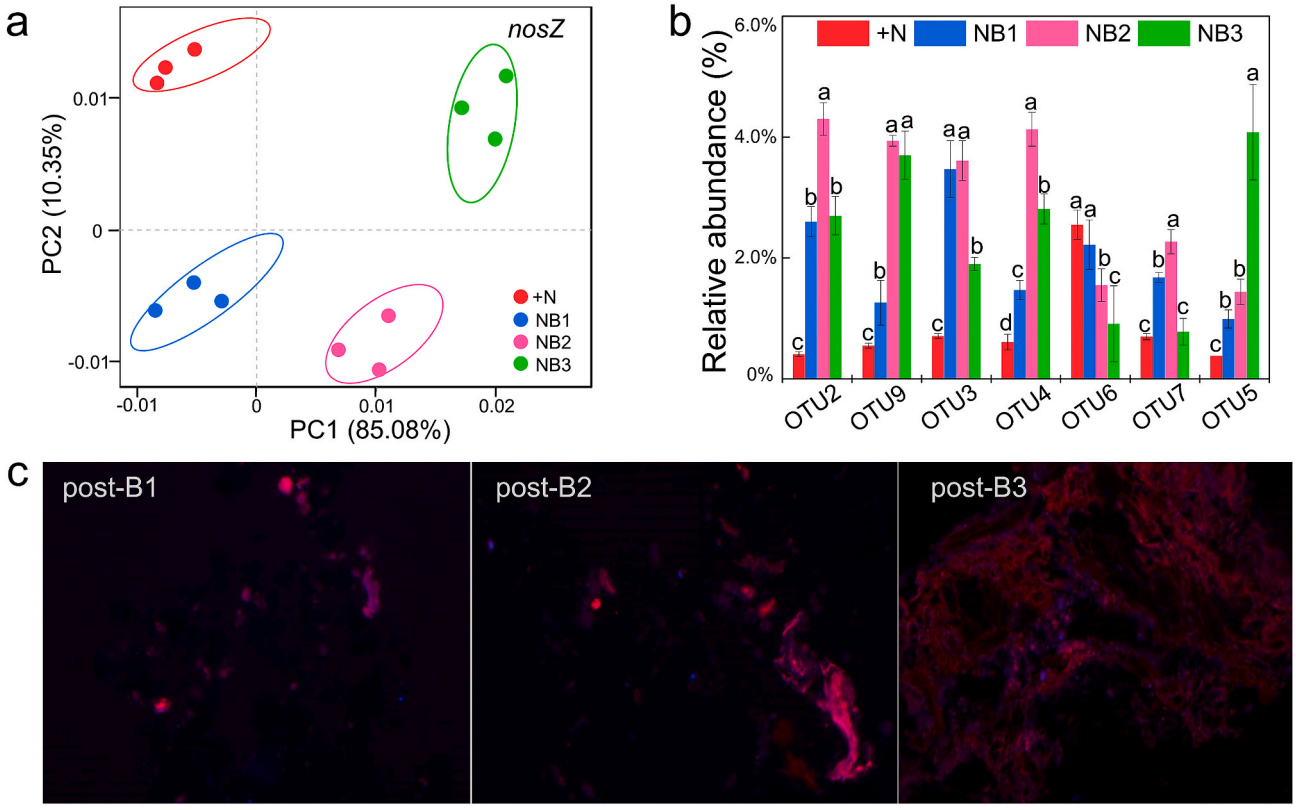

Fig. 4. Community composition based on *nosZ* gene in soil and localization on the biochar. Principal component analysis (PCA) of bacterial community based on *nosZ* gene in soil (a). Relative abundance of OTUs in soil (b). Statistically significant differences among experimental groups are represented by different lowercase letters ($p < 0.05$). Urea only (+N), and three kinds of SSA combined with urea (NB1, NB2 and NB3). Electron micrographs of FISH for OTU5 (red region) on different SSA biochar, Post-B1-3: represented B1-3 extraction from soil after 56 days incubation (c). (For interpretation of the references to color in this figure legend, the reader is referred to the Web version of this article.)

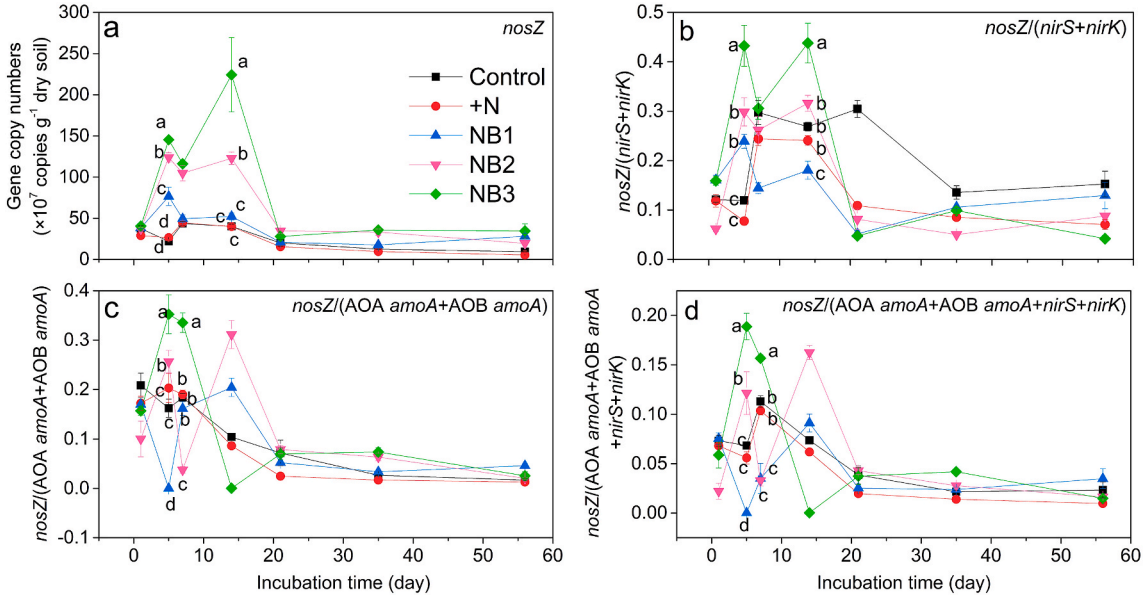

Fig. 5. Effects of biochar addition on the abundance of *nosZ* (a), *nosZ*/(*nirK* + *nirS*) (b), *nosZ*/(AOA *amoA* + AOB *amoA*) (c), and *nosZ*/(*nirK* + *nirS* + AOA *amoA* + AOB *amoA*) (d). Error bars are standard errors (n = 3). Statistically significant differences among experimental groups are represented by different lowercase letters ($p < 0.05$). No addition (Control), urea only (+N), and three kinds of SSA combined with urea (NB1, NB2 and NB3).

decreased N_2O emission. There are contradictory reports about the effect of biochar on N_2O emission, as some studies have reported that N_2O emission is stimulated by biochar addition (Shen et al., 2014; Lin et al., 2017) while others have reported its suppression (Thers et al., 2019), indicating that the mechanisms by which biochar affects N_2O emission are complex. N_2O flux peaked in the first 14 day, with a simultaneous

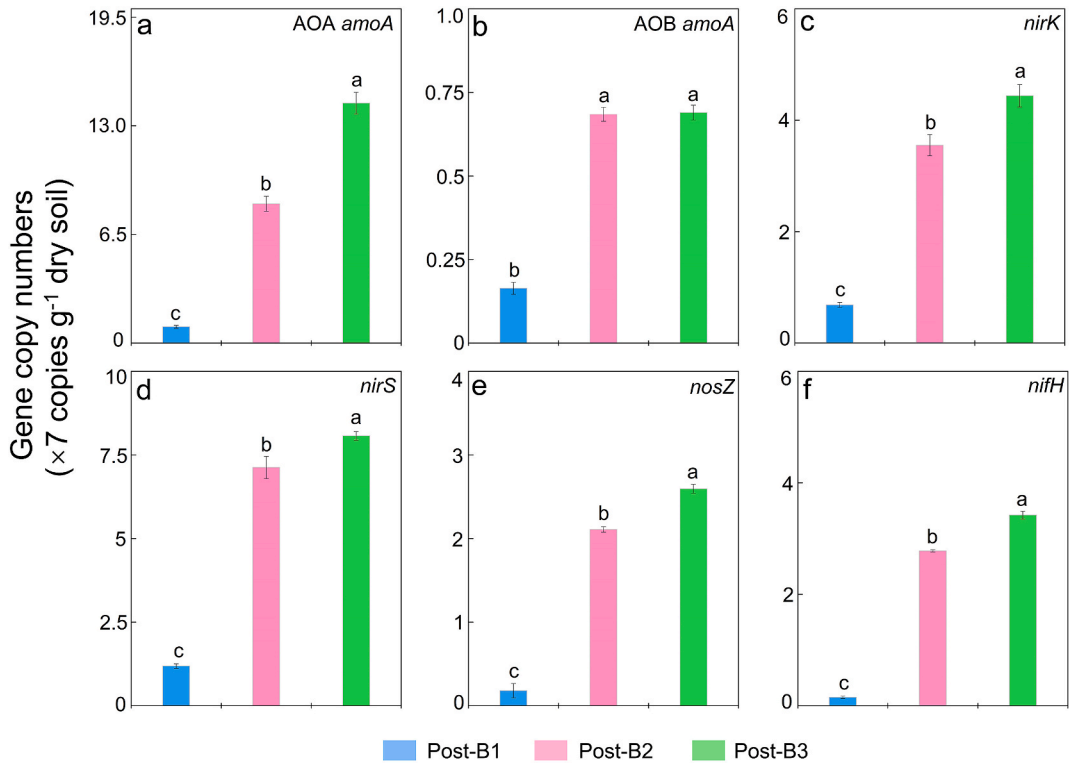

Fig. 6. The abundance of AOA *amoA* (a), AOB *amoA* (b), *nirK* (c), *nirS* (d), *nosZ* (e) and *nifH* (f) on different SSA biochar, Post-B1-3: represented B1-3 extraction from soil after 56 days incubation. Statistically significant differences among experimental groups are represented by different lowercase letters ($p < 0.05$).

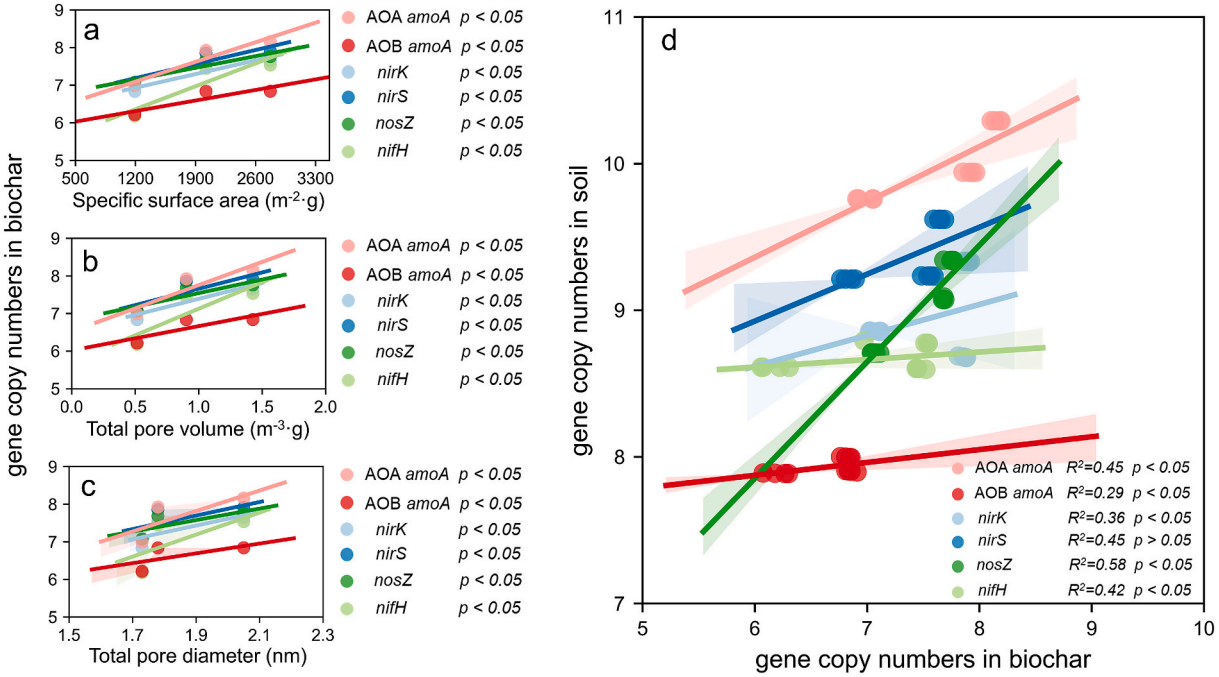

Fig. 7. The relationships between the abundance of AOA *amoA*, AOB *amoA*, *nirK*, *nirS*, *nosZ* and *nifH* with biochar specific surface area (a), total pore volume (b) and total pore diameter (c), and the relationships of these genes on biochar and in soil (d). Solid lines indicate the predicted relationships are significant ($p < 0.05$) based on linear regression estimated using ordinary least squares.

rapid decrease in NH_4^+ and increase in NO_3^-. Soil nitrification transforms NH_4^+ to NO_3^-, with N_2O emission being the by-product of nitrification (Bremner and Blackmer, 1978; Li et al., 2015), suggesting that nitrification is the predominant source of N_2O. The copy numbers of AOA *amoA* and AOB *amoA* were significantly higher in the biochar-treated soil than in the urea only-treated soil and positively ($p < 0.05$) correlated with N_2O flux. These findings are in accordance with those of field- and laboratory-based studies using different biochars and soils, where the *amoA* was responsible for stimulating N_2O emission from biochar-treated soil, which is the key step in the nitrification process

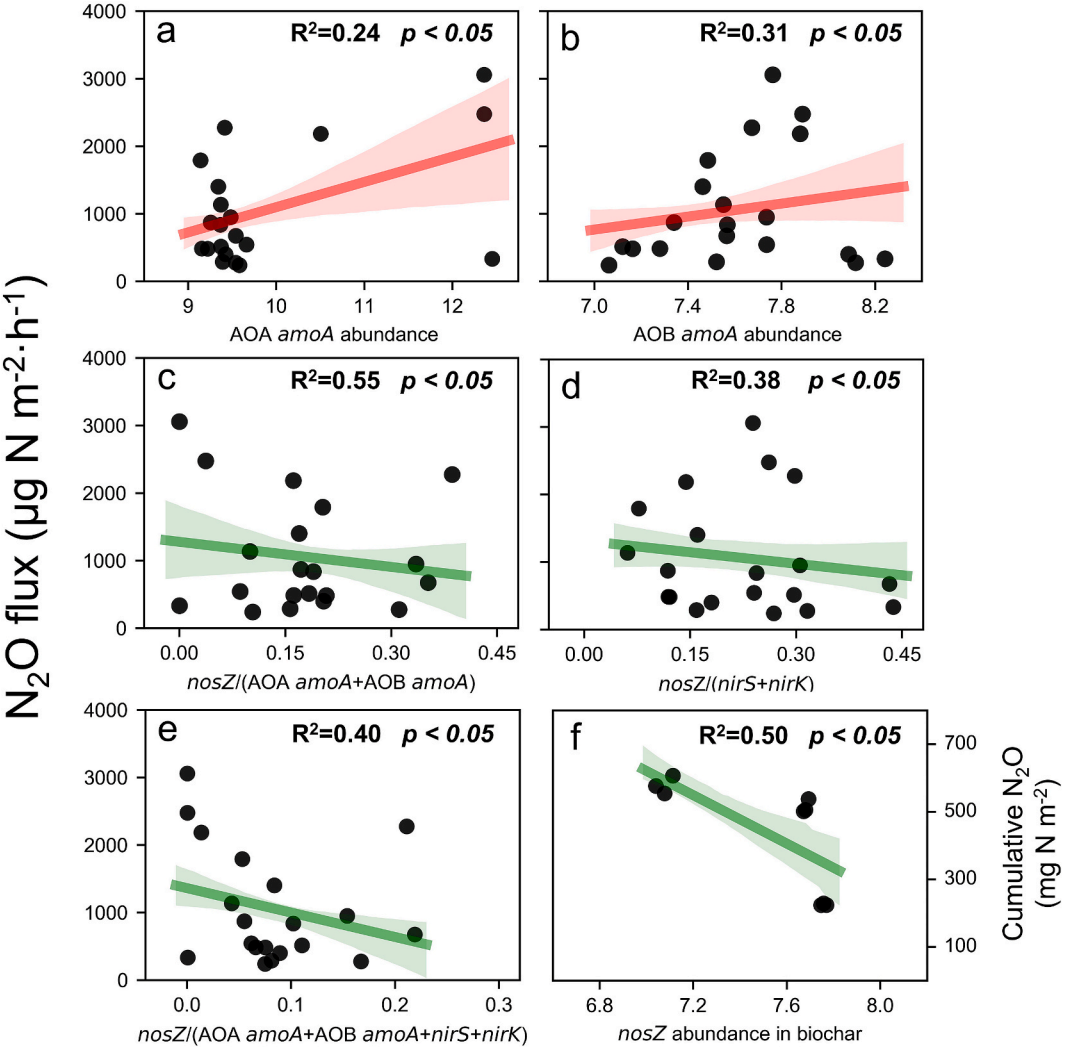

Fig. 8. The relationships between N_2O flux and AOA *amoA* copy numbers (a); AOB *amoA* copy numbers (b); ratio of *nosZ*/(AOA *amoA* + AOB *amoA*) (c); ratio of *nosZ*/(*nirK* + *nirS*) (d); *nosZ*/(AOA *amoA* + AOB *amoA* + *nirK* + *nirS*) in soil (e), and relationships between total N_2O and *nosZ* in biochar (f), as determined by regression analysis. Gene copy numbers were log transformed before regression analysis.

(Taketani and Tsai, 2010; Lin et al., 2017; Edwards et al., 2018). These results indicated that biochar stimulated N_2O emission by enhancing the copy numbers of the *amoA* of archaea and ammonia-oxidizing bacteria, compared with that of urea-only addition.

Biochars with larger SSAs significantly increased the copy number and ratio of *nosZ*. One-third of all denitrifiers, defined as *nirS*- or *nirK*-containing microorganisms, lack the genetic potential for N_2O reduction, and thus, are major contributors to microbial N_2O production (Jones et al., 2008; Philippot et al., 2011). Further, biochar addition decreased N_2O emission by enhancing the transformation of N_2O to N_2 by the N_2O-reducing bacteria (*nosZ*-encoded nitrous oxide reductase), which was the only known biological process for reducing N_2O to N_2 in the environment (Thomson et al., 2012). This finding confirms that biochar increased pH and *nosZ* gene copy number, as N_2O reductase (encoded by the *nosZ* gene) synthesis and assembly could be inhibited at low pH (Bergaust et al., 2010; Ducey et al., 2013; Van et al., 2014; Harter et al., 2014; Ji et al., 2020). In addition, our results confirmed that biochar changed (relative abundances of taxa) the bacterial community composition by increasing soil pH, NH_4^+, NO_3^-, C/N ratio, and cation exchange capacity. Further, it increased the relative abundances of microbes involved in nitrogen-cycling (such as Fibrobacteres, Nitrospirae, Gemmatimonadetes, Rokubacteria, Bacteroidetes, and Proteobacteria). Fibrobacteres can degrade cellulose (Ransom-Jones et al., 2012); Nitrospirae have high nitrification activity (Schramm et al., 1999); Gemmatimonadetes play a key role in assimilative and disassimilative nitrogen processes (Chee-Sanford et al., 2019); Rokubacteria contribute to secondary metabolite production (Crits-Christoph et al., 2018); and Bacteroidetes and Proteobacteria are positively correlated with soil ammonium nitrogen content (Yang et al., 2019). Biochar addition affects bacterial community composition by promoting the growth of bacteria with higher nitrogen metabolic-cycling abilities. Similarly, N_2O flux was significantly correlated with soil pH, NH_4^+, NO_3^-, C/N ratio, and cation exchange capacity, indicating that biochar may affect microbial processes by changing soil chemical properties and promoting the growth and activity of N_2O-reducing bacteria (containing *nosZ*), thereby affecting N_2O emission. The decreased N_2O emission was correlated with an increased abundance of *nosZ*; moreover, the ratio of *nosZ*/(*nirS* + *nirK*) was maximum in the soil treated with the biochar having the largest SSA, demonstrating that SSA > 2023 m^2 g^{-1} dramatically decreased N_2O emission by increasing *nosZ* abundance.

The composition of the bacterial community colonizing the biochar was affected by the SSA of biochar after 56 day of incubation. This finding is consistent with an earlier report by Dai et al. (2017), who found that differences in the composition of colonizing bacterial communities among different biochars are strongly influenced by the properties of the biochar (pH, surface area, and nutrient content). A

metagenomic study identified a gene cluster containing a urease operon with urea transport genes located downstream, as well as NH_4^+, NO_3^-, and NO_2^- transport genes in microbes growing on the biochar surface (Ye et al., 2017). The copy numbers (e.g., AOA *amoA*, *nirK*, *nirS*, *nosZ*, and *nifH*) increased with SSA of biochar up to 2773 $m^2\ g^{-1}$. Collectively, these contributed to the remarkable ability of biochar to adsorb NH_4^+ and NO_3^- *via* the numerous functional groups (carboxylic and hydroxyl groups, lactones, chromenes, ketones, and H-bonds) present on its surface (Kappler et al., 2014). In addition, our results confirmed that increased SSA (more pores with bigger diameters) of biochar could provide more living space for microbes. The pore of biochar might serve as a niche for nitrifiers and denitrifiers, thus promoting the selection of nitrogen-related functional genes (Yu et al., 2015; Saquing et al., 2016; Zhou et al., 2016). This selection process drives a series of microbial nitrogen processes, eventually leading to N_2O emission (Kammann et al., 2015; Schmidt et al., 2015; Su et al., 2019; Yuan et al., 2019). Our results supported the hypothesis that the copy numbers of functional genes of microbes (e.g., AOA *amoA*, *nirK*, *nirS*, *nosZ*, and *nifH*) colonizing biochar increase with pore volume and diameter, thereby affecting N_2O emission. For instance, the abundance of *nosZ* functional gene significantly increased with an increase in the SSA of biochar and led to a reduction in N_2O emission. Another potential mechanism may be that the significant increase in the abundance of the *amoA* on biochar can create anoxic microsites within the biochar particles by promoting heterotrophic microbial respiration and increasing O_2 consumption, leading to local anaerobiosis on the biochar surface and pores in the biochar particles (Van et al., 2009). Subsequently, complete versus incomplete denitrification ratio was increased by stimulating the activity and growth of N_2O-reducing microorganisms in the anoxic microsite environment, as N_2O reductase is more sensitive to O_2 than the enzymes involved in N_2O formation (Betlach and Tiedje, 1981; Jungkunst et al., 2006). In addition, biochar can function as an "electron shuttle," facilitating the transfer of electrons to soil denitrifiers. An increase in SSA enhances the electron shuttling properties of biochar, thereby promoting the reduction of N_2O to N_2 (Cayuela et al., 2014; Su et al., 2019; Yuan et al., 2019). These explain why the abundance of *nosZ* increased with an increase in the SSA of biochar up to 2773 $m^2\ g^{-1}$. The biochar with the largest SSA promoted the upregulation of the *nosZ* in soil, leading to a significantly decreased N_2O emission compared with the soils treated with biochars having smaller SSAs.

5. Conclusion

Increase in the SSA of biochar decreased N_2O emission by enhancing the abundance of *nosZ*. As we hypothesized, N_2O-reducing microbes colonizing on biochar were the key factor for the decrease in N_2O emissions. Biochar application changed soil properties, such as pH, C/N ratio, nitrogen availability (NO_3^- and NH_4^+), and cation exchange capacity, thereby affecting the diversity, structure, and function of total bacterial and N_2O-producing microbial communities. Using FISH and qPCR, we observed that the location of nitrogen functional microbes on the biochar, and their marker gene copy numbers in biochar and soil increased with SSA. The abundance of AOA *amoA* and AOB *amoA* increased in the biochar-treated soil and was positively related to N_2O flux, which could provide the best explanation for the increase in the N_2O emission with an increase in the SSA of biochar up to 2023 $m^2\ g^{-1}$. Moreover, the abundance of *nosZ* significantly increased with the SSA of biochar, and the ratio of *nosZ*/(*amoA* + *nirS* + *nirK*) was the highest in the soil treated with the biochar having the largest SSA and was linked to the pronounced reduction in N_2O emission, which was even lower than that in the urea only-treated soil. Our study has implications for optimizing biochar production for soil N_2O mitigation. Factors affecting the SSA of biochar and microbial colonization on biochar should be considered. However, the low amplification efficiency for the *nosZ* may be a limitation to this study; therefore, subsequent studies, such as metatranscriptomics or quantification of functional gene transcripts, may investigate functional gene expression to expand the results of this study. In addition, the results are based on a short-term incubation in the microcosm without growing plants, and the possible plant-soil biochar interaction under field conditions was not considered. For instance, in a field study by Castaldi et al. (2011), increased microbial activity due to wood-derived biochar amendment to soil were only transient. Thus, long-term field studies are needed to improve our understanding of the microbial colonization of biochar and its beneficial effects on N_2O mitigation.

Declaration of competing interest

The authors declare that they have no known competing financial interests or personal relationships that could have appeared to influence the work reported in this paper.

Acknowledgments

This study was supported in part by the National Key R&D Program of China (2017YFD0200100, 2017YFD0200104); the National Oilseed Rape Production Technology System of China; Double First-Class Construction Project of Hunan Agricultural University (kxk201801005); and Innovative Research Groups of the Natural Science Foundation of Hunan Province (2019JJ10003).

Appendix A. Supplementary data

Supplementary data to this article can be found online at https://doi.org/10.1016/j.soilbio.2021.108212.

References

Amann, R.I., 1995. In situ identification of micro-organisms by whole cell hybridization with rRNA-targeted nucleic acid probes. Molecular Microbial Ecology Manual 331–345.
Atkinson, C.J., Fitzgerald, J.D., Hipps, N.A., 2010. Potential mechanisms for achieving agricultural benefits from biochar application to temperate soils: a review. Plant and Soil 337 (1–2), 1–18.
Bergaust, L., Mao, Y., Bakken, L.R., Frostegard, A., 2010. Denitrification response patterns during the transition to anoxic respiration and posttranscriptional effects of suboptimal ph on nitrogen oxide reductase in paracoccus denitrificans. Applied and Environmental Microbiology 76 (19), 6387–6396.
Betlach, M.R., Tiedje, J.M., 1981. Kinetic explanation for accumulation of nitrite, nitric oxide, and nitrous oxide during bacterial denitrification. Applied and Environmental Microbiology 42, 1074–1084.
Bremner, J., Blackmer, A., 1978. Nitrous oxide: emission from soils during nitrification of fertilizer nitrogen. Science 199, 295–296.
Calvelo Pereira, R., Arbestain, M.C., Sueiro, M.V., Macia-Agullo, J.A., 2015. Assessment of the surface chemistry of wood-derived biochars using wet chemistry, Fourier transform infrared spectroscopy and X-ray photoelectron spectroscopy. Soil Research 53, 753–762.
Case, S.D., McNamara, N.P., Reay, D.S., Whitaker, J., 2012. The effect of biochar addition on N_2O and CO_2 emissions from a sandy loam soil–The role of soil aeration. Soil Biology and Biochemistry 51, 125–134.
Castaldi, S., Riondino, M., Baronti, S., Esposito, F.R., Marzaioli, R., Rutigliano, F.A., Vaccari, F.P., Miglierra, F., 2011. Impact of biochar application to a mediterranean wheat crop on soil microbial activity and greenhouse gas fluxes. Chemosphere 85 (9), 1464–1471.
Cayuela, M.L., Van Zwieten, L., Singh, B.P., Jeffery, S., Roig, A., Sánchez-Monedero, M. A., 2014. Biochar's role in mitigating soil nitrous oxide emissions: a review and meta-analysis. Agriculture, Ecosystems & Environment 191, 5–16.
Chee-Sanford, J., Tian, D., Sanford, R., 2019. Consumption of N_2O and other n-cycle intermediates by gemmatimonas aurantiaca strain T-27. Microbiology 165 (12).
Cornelissen, G., Rutherford, D.W., Arp, H.P.H., Dörsch, P., Kelly, C.N., Rostad, C.E., 2013. Sorption of pure N_2O to biochars and other organic and inorganic materials under anhydrous conditions. Environmental Science & Technology 47 (14), 7704–7712.
Crits-Christoph, A., Diamond, S., Butterfield, C.N., Thomas, B.C., Banfield, J.F., 2018. Novel soil bacteria possess diverse genes for secondary metabolite biosynthesis. Nature 558 (7710), 440.
Dai, Z., Barberan, A., Li, Y., Brookes, P.C., Xu, J., 2017. Bacterial community composition associated with pyrogenic organic matter (biochar) varies with pyrolysis temperature and colonization environment. mSphere 2 (2).
Ducey, T.F., Ippolito, J.A., Cantrell, K.B., Novak, J.M., Lentz, R.D., 2013. Addition of activated switchgrass biochar to an aridic subsoil increases microbial nitrogen cycling gene abundances. Applied Soil Ecology 65, 65–72.

Edgar, R.C., 2013. UPARSE: highly accurate OTU sequences from microbial amplicon reads. Nature Methods 10 (10), 996–998.
Edgar, R.C., Haas, B.J., Clemente, J.C., Quince, C., Knight, R., 2011. UCHIME improves sensitivity and speed of chimera detection. Bioinformatics 27 (16), 2194–2200.
Edwards, J.D., Pittelkow, C.M., Kent, A.D., Yang, W.H., 2018. Dynamic biochar effects on soil nitrous oxide emissions and underlying microbial processes during the maize growing season. Soil Biology and Biochemistry 122, 81–90.
Francis, C.A., Roberts, K.J., Michael Beman, J., Santoro, A.E., Oakley, B., 2005. Ubiquity and diversity of ammonia-oxidizing archaea in water columns and sediments of the ocean. Proceedings of the National Academy of Sciences of the United States of America 102, 14683e14688.
Gaby, J.C., Buckley, D.H., 2012. A comprehensive evaluation of PCR primers to amplify the *nifH* gene of nitrogenase. PloS One 7 (7), e42149.
Galloway, J.N., Townsend, A.R., Erisman, J.W., Bekunda, M., Cai, Z.C., Freney, J.R., 2008. Transformation of the nitrogen cycle: recent trends, questions, and potential solutions. Science 320, 889–892.
Harter, J., Krause, H.M., Schuettler, S., Ruser, R., Fromme, M., Scholten, T., Behrens, S., 2014. Linking N_2O emissions from biochar-amended soil to the structure and function of the N-cycling microbial community. The ISME Journal 8 (3), 660.
Henry, S., Baudoin, Ezékiel, López-Gutiérrez, Juan C., Martin-Laurent, F., Philippot, L., 2005. Quantification of denitrifying bacteria in soils by nirk gene targeted real-time pcr. Journal of Microbiological Methods 59 (3), 327–335.
Huang, M., Yang, L., Qin, H., Jiang, L., Zou, Y., 2013. Quantifying the effect of biochar addition on soil quality and crop productivity in Chinese rice paddies. Field Crops Research 154, 172–177.
Ji, C., Li, S., Geng, Y., Yuan, Y., Zhi, J., Yu, K., Zou, J., 2020. Decreased N_2O and NO emissions associated with stimulated denitrification following biochar amendment in subtropical tea plantations. Geoderma 365, 114223.
Jones, C.M., Stres, B., Rosenquist, M., Hallin, S., 2008. Phylogenetic analysis of nitrite, nitric oxide, and nitrous oxide respiratory enzymes reveal a complex evolutionary history for denitrification. Molecular Biology and Evolution 25 (9), 1955–1966.
Jungkunst, H.F., Freibauer, A., Neufeldt, H., Bareth, G., 2006. Nitrous oxide emissions from agricultural land use in Germany— a synthesis of available annual field data. Journal of Plant Nutrition and Soil Science 169 (3), 341–351.
Kammann, C.I., Schmidt, H.P., Messerschmidt, N., Linsel, S., Steffens, D., Müller, C., Joseph, S., 2015. Plant growth improvement mediated by nitrate capture in co-composted biochar. Scientific Reports 5, 11080.
Kappler, A., Wuestner, M.L., Ruecker, A., Harter, J., Halama, M., Behrens, S., 2014. Biochar as an electron shuttle between bacteria and Fe (III) minerals. Environmental Science and Technology 1, 339–344.
Keshri, J., Yousuf, B., Mishra, A., Jha, B., 2015. The abundance of functional genes, cbbL, nifH, amoA and apsA, and bacterial community structure of intertidal soil from Arabian Sea. Microbiological Research 175, 57–66.
Kloos, K., Mergel, A., Rösch, Christopher, Bothe, H., 2001. Denitrification within the genus azospirillum and other associative bacteria. Functional Plant Biology 28 (9), 991–998.
Laird, D.A., Fleming, P., Davis, D.D., Horton, R., Wang, B., Karlen, D.L., 2010. Impact of biochar amendments on the quality of a typical Midwestern agricultural soil. Geoderma 158 (3–4), 443–449.
Li, J., Nedwell, D.B., Beddow, J., Dumbrell, A.J., McKew, B.A., Thorpe, E.L., Whitby, C., 2015. *amoA* gene abundances and nitrification potential rates suggest that benthic ammonia-oxidizing bacteria and not archaea dominate N cycling in the Colne Estuary, United Kingdom. Applied and Environmental Microbiology 81 (1), 159–165.
Liang, C., Li, Z., Dai, S., 2008. Mesoporous carbon materials: synthesis and modification. Angewandte Chemie International Edition 47 (20), 3696–3717.
Lin, Y., Ding, W., Liu, D., He, T., Yoo, G., Yuan, J., Fan, J., 2017. Wheat straw-derived biochar amendment stimulated N_2O emissions from rice paddy soils by regulating the *amoA* genes of ammonia-oxidizing bacteria. Soil Biology and Biochemistry 113, 89–98.
Lin, Y., Munroe, P., Joseph, S., Kimber, S., Van Zwieten, L., 2012. Nanoscale organo-mineral reactions of biochars in ferrosol: an investigation using microscopy. Plant and Soil 357, 369–380.
Liu, X., Liao, J., Song, H., Yang, Y., Guan, C., Zhang, Z., 2019. A biochar-based route for environmentally friendly controlled release of nitrogen: urea-loaded biochar and bentonite composite. Scientific Reports 9 (1).
Liu, Y.R., Delgado-Baquerizo, M., Trivedi, P., He, J.Z., Singh, B.K., 2016. Species identity of biocrust-forming lichens drives the response of soil nitrogen cycle to altered precipitation frequency and nitrogen amendment. Soil Biology and Biochemistry 96, 128–136.
Loftfield, N., Flessa, H., Augustin, J., Beese, F., 1997. Automated gas chromatographic system for rapid analysis of the atmospheric trace gases methane, carbon dioxide, and nitrous oxide. Journal of Environmental Quality 26 (2), 560–564.
Lu, S., Lepo, J.E., Song, H.X., Guan, C.Y., Zhang, Z.H., 2018. Increased rice yield in long-term crop rotation regimes through improved soil structure, rhizosphere microbial communities, and nutrient bioavailability in paddy soil. Biology and Fertility of Soils 54 (8), 909–923.
Marusina, A.I., Boulygina, E.S., Kuznetsov, B.B., Tourova, T.P., Kravchenko, I.K., Gal'chenko, V.F., 2001. A system of oligonucleotide primers for the amplification of nifH genes of different taxonomic groups of prokaryotes. Microbiology 70 (1), 73–78.
Oksanen, J., Blanchet, F.G., Friendly, M., Kindt, R., Legendre, P., McGlinn, D., Minchin, P.R., O'Hara, R.B., Simpson, G.L., Solymos, P., Stevens, M.H., 2016. Vegan: Community Ecology Package. R Package Version 2.4–1.
Pernthaler, A., Pernthaler, J., 2007. Fluorescence in situ hybridization for the identification of environmental microbes. In: Protocols for Nucleic Acid Analysis by Nonradioactive Probes. Humana Press, pp. 153–164.
Philippot, L., Andert, J., Jones, C.M., Bru, D., Hallin, S., 2011. Importance of denitrifiers lacking the genes encoding the nitrous oxide reductase for N_2O emissions from soil. Global Change Biology 17 (3), 1497–1504.
Ransom-Jones, E., Jones, D.L., McCarthy, A.J., McDonald, J.E., 2012. The Fibrobacteres: an important phylum of cellulose-degrading bacteria. Microbial Ecology 63 (2), 267–281.
Ravishankara, A.R., Daniel, J.S., Portmann, R.W., 2009. Nitrous oxide (N_2O): the dominant ozone-depleting substance emitted in the 21st century. Science 326 (5949), 123–125.
Taketani, Rodrigo Gouvêa, Tsai, S.M., 2010. The influence of different land uses on the structure of archaeal communities in amazonian anthrosols based on 16s rrna and amoa genes. Microbial Ecology 59 (4), 734–743.
Rotthauwe, J.H., Witzel, K.P., Liesack, W., 1997. The ammonia monooxygenase structural gene *amoA* as a functional marker: molecular fine-scale analysis of natural ammonia-oxidizing populations. Applied and Environmental Microbiology 63, 4704e4712.
Ruser, R., Schilling, R., Steindl, H., Flessa, H., Beese, F., 1998. Soil compaction and fertilization effects on nitrous oxide and methane fluxes in potato fields. Soil Science Society of America Journal 62 (6), 1587–1595.
Saquing, J.M., Yu, Y., Chiu, P.C., 2016. Wood-derived black carbon (biochar) as a microbial electron donor and acceptor. Environmental Science and Technology Letters 3, 62–66.
Schmidt, H., Pandit, B., Martinsen, V., Cornelissen, G., Conte, P., Kammann, C., 2015. Fourfold increase in pumpkin yield in response to low-dosage root zone application of urine-enhanced biochar to a fertile tropical soil. Agriculture 5 (3), 723–741.
Schöler, A., Jacquiod, S., Vestergaard, G., Schulz, S., Schloter, M., 2017. Analysis of soil microbial communities based on amplicon sequencing of marker genes. Biology and Fertility of Soils 53, 485–489.
Schramm, A., de Beer, D., van den Heuvel, J.C., Ottengraf, S., Amann, R., 1999. Microscale distribution of populations and activities of Nitrosospira and Nitrospira spp. along a macroscale gradient in a nitrifying bioreactor: quantification by in situ hybridization and the use of microsensors. Applied and Environmental Microbiology 65, 3690e3696.
Shcherbak, I., Millar, N., Robertson, G.P., 2014. Global meta-analysis of the nonlinear response of soil nitrous oxide (N_2O) emissions to fertilizer nitrogen. Proceedings of the National Academy of Sciences 111 (25), 9199–9204.
Shen, J., Tang, H., Liu, J., Wang, C., Li, Y., Ge, T., Jones, D.L., Wu, J., 2014. Contrasting effects of straw and straw-derived biochar additions on greenhouse gas emissions within double rice cropping systems. Agriculture, Ecosystems & Environment 188, 264e274.
Spokas, K.A., Baker, J.M., Reicosky, D.C., 2010. Ethylene: potential key for biochar amendment impacts. Plant and Soil 333 (1–2), 443–452.
Su, X., Wang, Y., He, Q., Hu, X., Chen, Y., 2019. Biochar remediates denitrification process and N_2O emission in pesticide chlorothalonil-polluted soil: role of electron transport chain. Chemical Engineering Journal 370, 587–594.
Thers, H., Djomo, S.N., Elsgaard, L., Knudsen, M.T., 2019. Biochar potentially mitigates greenhouse gas emissions from cultivation of oilseed rape for biodiesel. The Science of the Total Environment 671 (JUN.25), 180–188.
Thomson, A.J., Giannopoulos, G., Pretty, J., Baggs, E.M., Richardson, D.J., 2012. Biological sources and sinks of nitrous oxide and strategies to mitigate emissions. Philosophical Transactions of the Royal Society B: Biological Sciences 367 (1593), 1157–1168.
Throback, I.N., Enwall, K., Jarvis, A., Hallin, S., 2004. Reassessing PCR primers targeting nirS, nirK and nosZ genes for community surveys of denitrifying bacteria with DGGE. FEMS Microbiology Ecology 49 (3), 401–417.
Tian, H., Yang, J., Xu, R., Lu, C., Canadell, J.G., Davidson, E.A., Gerber, S., 2019. Global soil nitrous oxide emissions since the preindustrial era estimated by an ensemble of terrestrial biosphere models: magnitude, attribution, and uncertainty. Global Change Biology 25 (2), 640–659.
Van, Zwieten L., Singh, B., Joseph, S., Kimber, S., Cowie, A., Chan, K., 2009. Biochar and emissions of Non-CO_2 greenhouse gases from soil. In: Lehmann, J., Joseph, S. (Eds.), Biochar for Environmental Management Science and Technology. Earthscan, London, UK, pp. 227–249.
Van, Zwieten L., Kimber, S., Morris, S., Downie, A., Berger, E., Rust, J., Scheer, C., 2010. Influence of biochars on flux of N_2O and CO_2 from Ferrosol. Soil Research 48 (7), 555–568.
Van, Zwieten L., Singh, B.P., Kimber, S.W.L., Murphy, D.V., Macdonald, L.M., Rust, J., Morris, S., 2014. An incubation study investigating the mechanisms that impact N_2O flux from soil following biochar application. Agriculture, Ecosystems & Environment 191, 53–62.
Vestergaard, G., Schulz, S., Schöler, A., Schloter, M., 2017. Making big data smart—how to use metagenomics to understand soil quality. Biology and Fertility of Soils 53 (5), 479–484.
Wang, Q., Zhou, F., Shang, Z., Ciais, P., Winiwarter, W., Jackson, R.B., Tao, S., 2020. Data-driven estimates of global nitrous oxide emissions from croplands. National Science Review 7 (2), 441–452.
Wendeberg, & A., 2010. Fluorescence in situ hybridization for the identification of environmental microbes. Cold Spring Harbour Protocols 2010 (1).
Xu, H.J., Wang, X.H., Li, H., Yao, H.Y., Su, J.Q., Zhu, Y.G., 2014. Biochar impacts soil microbial community composition and nitrogen cycling in an acidic soil planted with rape. Environmental Science & Technology 48 (16), 9391–9399.
Xu, S., Feng, S., Sun, H., Wu, S., Zhuang, G., Deng, Y., Zhuang, X., 2018. Linking N_2O emissions from biofertilizer-amended soil of tea plantations to the abundance and

structure of N_2O-reducing microbial communities. Environmental Science & Technology 52 (19), 11338–11345.
Yanai, Y., Toyota, K., Okazaki, M., 2007. Effects of charcoal addition on N_2O emissions from soil resulting from rewetting air-dried soil in short-term laboratory experiments. Soil Science & Plant Nutrition 53 (2), 181–188.
Yang, X.C., Han, Z.Z., Ruan, X.Y., Chai, J., Jiang, S.W., Zheng, R., 2019. Composting swine carcasses with nitrogen transformation microbial strains: succession of microbial community and nitrogen functional genes. The Science of the Total Environment 688, 555–566.
Ye, J., Joseph, S.D., Ji, M., Nielsen, S., Mitchell, D.R., Donne, S., Thomas, T., 2017. Chemolithotrophic processes in the bacterial communities on the surface of mineral-enriched biochars. The ISME Journal 11 (5), 1087–1101.
Yu, L., Yuan, Y., Tang, J., Wang, Y., Zhou, S., 2015. Biochar as an electron shuttle for reductive dechlorination of pentachlorophenol by Geobacter sulfurreducens. Scientific Reports 5, 16221.
Yuan, H., Zhang, Z., Li, M., Clough, T., Wrage-Mönnig, N., Qin, S., Zhou, S., 2019. Biochar's role as an electron shuttle for mediating soil N_2O emissions. Soil Biology and Biochemistry 133, 94–96.
Zhang, A., Cui, L., Pan, G., Li, L., Hussain, Q., Zhang, X., Zheng, J., Crowley, D., 2010. Effect of biochar addition on yield and methane and nitrous oxide emissions from a rice paddy from Tai Lake plain, China. Agriculture, Ecosystems & Environment 139, 469–475.
Zhou, G., Yang, X., Li, H., Marshall, C.W., Zheng, B., Yan, Y., Su, J., Zhu, Y., 2016. Electron shuttles enhance anaerobic ammonium oxidation coupled to iron (III) reduction. Environmental Science and Technology 50, 9298–9307.
Zhu, T., Zhang, J., Huang, P., Suo, L., Wang, C., Ding, W., Hu, Z., 2015. N_2O emissions from banana plantations in tropical China as affected by the application rates of urea and a urease/nitrification inhibitor. Biology and Fertility of Soils 51 (6), 673–683.